Macromolecules

ARTICLE

pubs.acs.org/Macromolecules

Radical Photopolymerization in Miniemulsions. Fundamental Investigations and Technical Development

Pablo A. Hoijemberg,[‡,†] Abraham Chemtob,[‡,*] Céline Croutxé-Barghorn,[‡] Julien Poly,[‡] and André M. Braun[§]

[‡]Laboratory of Photochemistry and Macromolecular Engineering, CNRS, ENSCMu University of Haute-Alsace, 3 rue Alfred Werner 68093 Mulhouse Cedex, France

[§]Engler-Bunte-Institute, Karlsruhe Institute of Technology, 76131 Karlsruhe, Germany

ABSTRACT: A photochemical means to convert acrylate monomer emulsions into polymer nanolatexes has been explored using radical miniemulsion photopolymerization. Our aim is to offer a complete overview through a stepwise mechanistic investigation, addressing first the key aspect of the electronic excitation of the photoinitiator in monomer miniemulsions and ending with the implementation of a photochemical reactor. In a first step, the photon flux absorbed by different photochemical initiators was investigated as a function of the miniemulsion droplet size. A series of miniemulsion polymerizations were also performed and the effects of the primary experimental parameters on the reactions kinetics, molar masses, and colloidal properties were assessed. As expected, droplet size, incident photon flux, and the nature of the photochemical initiator were found to be the primary reaction parameters. Finally, miniemulsion polymerizations were performed in an annular photochemical reactor in batch and semibatch processes.

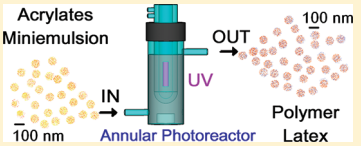

INTRODUCTION

Applied polymer preparations are largely focused on free-radical polymerizations owing to the robustness of the products and the compatibility of the techniques with a variety of process conditions. In compliance with new environmental regulations, important research efforts concern formulations in which no or only low contents of volatile organic compounds (VOC) are used in energy-saving processes producing minimal waste. Among a number of proposed alternatives, radical polymerization in dispersed aqueous media has gained special attention. Up to the present, all emulsion polymerization processes implemented industrially rely on thermal or redox initiators, mainly in conventional stirred tank reactors. Despite the technical performance and the economic success of those procedures, pressure remains to improve performance and environmental compatibility. Within this context, photochemical means to convert monomer emulsions into polymer latexes have yet to be explored.

The potential of the photochemical polymerization has so far only been exploited for the production of cross-linked static films (1−1000 μm).[1] Generally, such photochemical polymerization processes are solvent-free and require energy efficient curing only in restricted domains (*e.g.*, coating, adhesives, dental restoration, stereolithography, and ink drying).[2] Little progress has been made so far on the use of photochemical means to synthesize linear, high-molar mass polymers in aqueous and even in organic media. The pioneering work of Melville et al. in the 1950s dealt with the photochemical polymerization of vinyl and acrylate monomers.[3] Later, Ryan and Gormley described a somewhat larger scale polymerization of dissolved isopropyl acrylate using four identical UV lamps mounted outside a 500 mL glass container.[4] Following such early experiments, a couple of patents were released in the 1980s, describing photochemical polymerizations in bulk or in solution and disclosing the use of irradiated conveyor belts,[5,6] but their exploitation was mainly prevented by problems of up-scaling and homogeneity of irradiation. For bulk systems and organic solutions, process intensification was attempted by some groups proposing a range of well-designed photochemical reactors, e.g., spinning disk reactor,[7,8] continuous rotating spiral conveyor,[9] or falling film reactor.[10] Among the most promising approaches, Braun et al. designed a tubular photochemical reactor with negative irradiation geometry to prepare PMMA-prepolymers in a bulk batch procedure using excimer radiation of variable frequency.[11,12] A similar equipment but with continuous irradiation was used by Jachuck et al. for the photochemical polymerization of *n*-butyl acrylate in solution.[13] Up to the present, no equivalent investigation was found for emulsion polymerization, although the use of dispersed systems would provide a number of improvements, e.g. processes without the use of organic solvents conducted at ambient temperature, controlled and low viscosities during reaction time, higher rates of polymerization due to reaction compartmentalization in confined droplets, etc.

The feasibility of emulsion-based photochemical polymerizations was tested earlier with simple bench equipments. These investigations implied mainly polymerizations in microemulsions[14−25] or micelles,[26−34] but other work dealt with emulsion,[35−38] dispersion,[39,40] miniemulsion,[41−43] and suspension[44,45] polymerizations under special experimental conditions. A photochemically initiated polymerization in miniemulsion could provide a number of advantages with respect to the other techniques. Monomer miniemulsions are defined as kinetically stable submicrometer

Received: July 29, 2011
Revised: September 28, 2011
Published: October 25, 2011

monomer-in-water dispersions,[46] with droplet sizes comprised between 50 and 500 nm. In contrast to emulsion polymerization, the high number of droplets generated is intended to avoid the formation of micelles and thus maximize the fraction of polymer particles generated by droplet nucleation. Ideally, the high initiation rate inherent in the use of photochemical initiators is likely to affect positively the overall polymerization kinetics. With a fast nucleation and a polymerization rate higher than that of monomer mass transport, it is also expected that the photochemical process will contribute to increase the proportion of nucleated droplets. Increased temperatures that are known to enhance coalescence (droplet−droplet, droplet−particle) and coagulation (particle−particle) are however not needed in a photochemical process. Radical photochemical initiators exhibit a high quantum yield of homolysis generating the free radicals needed to trigger polymerization of vinyl monomers. Nonetheless, this initiation depends however strongly on the incident light intensity and on the photon flux absorbed by the initiator. Consequently, increased scattering properties of heterogeneous reaction systems will diminish the rate of initiation. In miniemulsion, attenuation by scattering might be minimized if the mean diameter of the droplets remains below 100 nm. Recent reports on photopolymerizations in miniemulsions include the works of Lacroix-Desmaze et al. on a specific iodine transfer photopolymerization in presence of a macrophotoiniferter[41] (acting as an initiator, transfer agent, and terminator) and the preparation of polyacrylate latexes encapsulating gold[42] or magnetic[43] nanoparticles. Beside these rare photochemical processes, ultrasound,[47] microwave[48] and γ-ray[49−51] initiated polymerizations in miniemulsions were also reported lately.

Following a number of exploring experimental series,[52] we are aiming at a more detailed discussion of the radiation-induced polymerization in miniemulsions by a stepwise mechanistic investigation, starting with the electronic excitation of the initiator in an acrylate monomer miniemulsion and ending with the design and implementation of an appropriate photochemical reactor. In a first step, the photon flux absorbed by different photochemical initiators was investigated as a function of the mean diameter of the droplets of the miniemulsion. In a second step, a series of photochemical polymerizations were performed in miniemulsion, and the effects of the primary experimental parameters on the reactions kinetics were assessed by real-time FT-NIR monitoring. As expected, droplet size, incident photon flux and the nature of the photochemical initiator were found to be the primary reaction parameters. Finally, miniemulsion polymerizations were performed in a photochemical reactor in batch and semibatch processes.

EXPERIMENTAL SECTION

Materials. All miniemulsions were prepared with Milli-Q water. Sodium dodecyl sulfate (SDS, Aldrich) was used as the surfactant, and hexadecane (Aldrich) was added to the miniemulsion formulation as costabilizer. Technical grade monomers: butyl acrylate (BA), methyl methacrylate (MMA), and acrylic acid (AA) were supplied by Aldrich and used without further purification. The following photochemical initiators were provided by Ciba Specialty Chemicals: 2-methyl-1[4-(methylthio)phenyl]-2-morpholinopropan-1-one (Irgacure 907, **1**), 1-[4-(2-hydroxyethoxy)-phenyl]-2-hydroxy-2-methyl-1-propane-1-one (Irgacure 2959, **2**), 2-benzyl-2-dimethylamino-1-(4-morpholinophenyl)-butanone-1 (Irgacure 369, **3**), 2,2-dimethoxy-1,2-diphenylethan-1-one (DMPA or Irgacure 651, **4**) and phosphine oxide phenyl bis(2,4,6-trimethyl benzoyl) (BAPO or Irgacure 819, **5**).

Scheme 1. Schematic Diagram of the Lab Bench Photoreactor

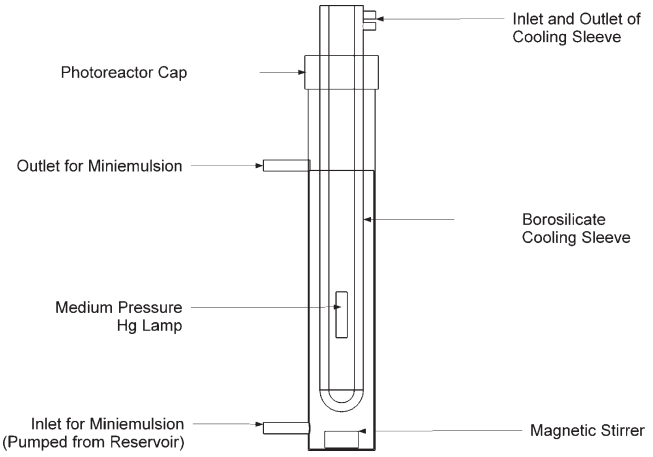

Preparation of Monomer Miniemulsions. The generation of monomer miniemulsion is induced by high energy input homogenization provided by a high shear device (ultrasonication, high-pressure homogenizer, etc.). In order to stabilize the miniemulsion efficiently against diffusional degradation (Ostwald ripening) and coalescence, the monomer nanodroplets must comprise a costabilizer of low molecular weight and limited water-solubility.[46] In a typical preparation, an organic phase was prepared by mixing hexadecane as the costabilizer (4% w/$w_{monomer}$) and a lipophilic photochemical initiator (**1**, **3**, **4** or **5**, 2% w/$w_{monomer}$) with the monomer mixture of BA, MMA and AA with 49.5, 49.5 and 1% w/w, respectively. The aqueous phase was prepared separately by dissolving 1.5% w/w_{water} of SDS in Milli-Q water. In cases, where a water-soluble photochemical initiator was used, **2** (2% w/$w_{monomer}$) was preliminarily dissolved in water. Both phases were mixed during at least 10 min using a magnetic stirrer at 600 rpm. The coarse emulsion was subsequently sonicated (Branson Sonifier 450 (450 W/L)) during variable times while maintaining the agitation, in order to obtain the desired average droplet size. This procedure yielded a constant organic phase content φ_{org} of the miniemulsion of 17% w/w_{total}.

Photopolymerizations in Miniemulsion. • *Photochemical Polymerization in a Spectroscopic Cell (1 mm Thickness).* In a typical procedure, the photochemical polymerization of the air-saturated monomer miniemulsion was carried in a capped quartz cylindrical cell (1 mm thick, 19 mm diameter) without purging and stirring. UV/vis-radiation was produced by a Hg−Xe lamp (Hamamatsu L8252, 200 W, reflector at 365 nm) and coupled with a flexible light-guide. The end of the optical guide was placed at a distance of 4.2 cm from the cell and directed at an incident angle of 90° onto the cell window. The exitance (E_p) could be varied from 4 to 200 mW/cm^2. This setup was used for the kinetic analysis of the photopolymerization by real-time Fourier transform near-infrared spectroscopy (RT-FTNIR). In all experiments, a 300 nm cutoff filter was placed between the lamp and the light-guide to avoid interfering absorption by the monomers.

• *Photopolymerization in a Lab Photoreactor.* An immersion-type photochemical reactor (UV-Consulting Peschl) equipped with a 150 W medium pressure Hg arc (Heraeus Noblelight TQ150, arc length: 4.1 cm, Scheme 1) was used for preparative experiments. The lamp was contained in a quartz tube and placed into a borosilicate sleeve for internal water cooling, the device also filtering incident radiation of wavelengths below 300 nm. The optical path of the reactor unit was 9 mm.

In batch mode, the reactor was filled with 400 mL of freshly sonicated monomer miniemulsion that was stirred with a magnetic stirrer. The reaction system was not purged before or during irradiation. During

irradiation, samples were withdrawn for kinetic measurements as well as for the characterization of molar masses and colloidal properties. In semibatch mode, the miniemulsion was circulated between the reactor and a reservoir (500 mL) by means of a gear pump (Ismatec Reglo-Z, with pump head Z-181) with a slow flow of 4.2 mL/min throughout the irradiation.

Methods of Analysis. Droplet (d_d) and particle (d_p) size (z-average diameters) were determined by dynamic light scattering (DLS) using a Zetasizer nano ZS (Malvern Instruments). For this purpose, samples of the miniemulsions were diluted 10 times their volume with their corresponding aqueous phase, and measurements were conducted within 5 min of sample preparation, mainly to avoid droplet destabilization. The ratio between the number density of particles and the initial number density of droplets (N_p/N_d) was also determined from size data. However, these values might lack precision, taking into account the limits of error of the DLS analysis, and the third power of the resulting values to be used to calculate N_d and N_p. UV/vis-absorption spectra were taken with a Varian Cary 4000 spectrophotometer, the miniemulsions being placed in a quartz cell of 0.1 mm optical path. Overall acrylate conversion was followed by RT-FTNIR spectroscopy in transmission (IFS/66, Bruker). In a typical experiment, the sample in the spectroscopic cell was exposed simultaneously to UV-radiation, initiating polymerization, and to the analyzing NIR-beam, monitoring continuously the decrease of absorbance of the acrylate function at 6170 cm^{-1}. RT-FTIR is a widespread technique generally used to monitor the ultrafast photocross-linking of static films.[1] In the present study, the RT-FTNIR process monitoring was enabled by the low liquid film thickness (1 mm) and its moderate backscattering properties. The NIR spectral region was chosen owing to the low absorption of water within this spectral domain of analysis. The linear part of the evolution of conversion versus reaction time allowed the determination of initial rates of polymerization (r_p, (L mol^{-1} s^{-1})) and the calculation of the corresponding $r_p/[M]_0$ values (s^{-1}), with $[M]_0$ representing the initial monomer concentration. Varying polychromatic exitance (E_p) and the photochemical initiator (PI), but keeping all other process variables constant, relative rates of polymerization (eq 1) could be calculated, taking the initial rate of acrylate polymerization initiated by **1** of defined concentration and under maximum polychromatic exitance (200 mW/cm^2) as a reference.

$$r_p^{rel} = \frac{r_p^{Ep}(PI)}{r_p^{200mW/cm^2}(\mathbf{1})} \quad (1)$$

After purification by precipitation in added methanol, the polymers were dissolved in THF (concentrations ranging from 5 to 10 mg/mL) and the solutions filtered through PTFE membranes (0.45 μm, Millex). Samples were subsequently analyzed by means of size exclusion chromatography (SEC, pump: Shimadzu LC-20AD, autosampler: Shimadzu SIL-20A, oven: Shimadzu CTO-20A (30 °C), columns: PLgel 10 μm guard (50 × 7.5 mm) and two PLgel 5 μm MIXED-C (300 × 7.5 mm) (Polymer Laboratories), eluent: THF (1.0 mL/min), detectors: Shimadzu RID-10A (refractive index) and Viscotek 270 Dual Detector (light scattering). Molar masses were determined by the multidetection method using OmniSEC Viscotek software (version 4.6.1). The branched structure of the formed polyacrylates is likely to cause complications in the interpretation of the SEC data.

RESULTS AND DISCUSSION

Except for the presence of an α-aminoacetophenone- (**1**-) based PI that replaces a thermal initiator, the composition of the starting monomer miniemulsion is similar to that reported for thermally activated processes (BA/MMA/AA, 49.5/49.5/1% wt, stabilized with SDS and hexadecane). In this type I radical initiation, electronic excitation of the benzoyl chromophore leads

Scheme 2. Photolysis of the α-Aminoacetophenone Type PI 1

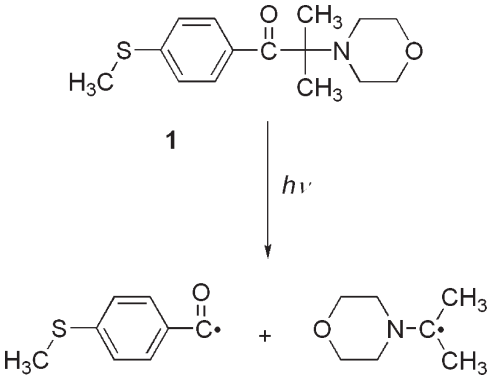

to the homolysis of the bond adjacent to the carbonyl function (α-cleavage), as displayed in Scheme 2. As a result, benzoyl and α-substituted alkyl radicals are generated, both being instrumental in the initiation step.[53] Most of the commercially available photochemical initiators are lipophilic and can be readily dissolved in the monomer (organic) phase of a miniemulsion. This is in sharp contrast with emulsion polymerizations, where water-soluble initiators are typically used.

I. Spectrophotometric Characterization of Monomer Miniemulsions Containing a Photochemical Initiator. A photochemical reaction in a heterogeneous reaction system is affected by scattering phenomena that, depending on the size of droplets or particles, will affect the incident photon flux interacting with the photochemically reactive compound dissolved in these droplets. An increase in droplet diameter, within the scope of this work, will lead to a stronger scattering effect. In heterogeneous systems, absorption spectra rely not only on the absorption of incident radiation by dissolved compounds but also on the diminution of the internal transmittance by scattering. Under these conditions, eqs 2 and 3 (Lambert−Beer's law), valid for ideal solutions,

$$\sum_\lambda P_{0,\lambda} = \sum_\lambda (P_{a,\lambda} + P_{t,\lambda}) \quad (2)$$

where

$\Sigma_\lambda P_{0,\lambda}$: incident polychromatic photon flux [einstein L^{-1} s^{-1}]
$\Sigma_\lambda P_{a,\lambda}$: absorbed polychromatic photon flux [einstein L^{-1} s^{-1}]

$$\sum_\lambda P_{a,\lambda} = \sum_\lambda P_{0,\lambda}(1 - 10^{-[PI]\varepsilon_{PI,\lambda}l}) \quad (3)$$

where

[PI]: concentration of PI [mol^{-1} L]
$\varepsilon_{PI,\lambda}$: molar absorption coefficient of PI at the wavelength of excitation (λ) [L mol^{-1} cm^{-1}]
l: optical path length [cm]
$\Sigma_\lambda P_{t,\lambda}$: nonabsorbed (transmitted) polychromatic photon flux [einstein L^{-1} s^{-1}]

and must be modified for the fraction of incident radiation that will be scattered (eq 4.

$$\sum_\lambda P_{0,\lambda} = \sum_\lambda (P'_{a,\lambda} + P_{s,\lambda} + P_{t,\lambda}) \quad (4)$$

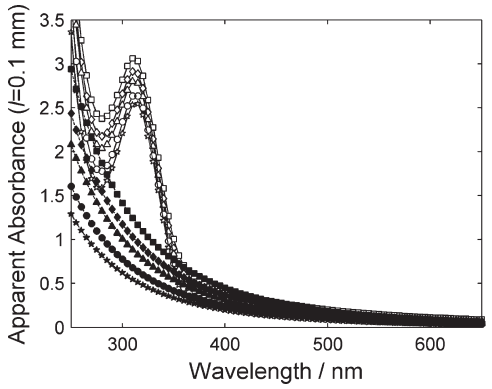

Figure 1. Absorption spectra of monomer acrylate miniemulsions of different average droplet sizes (φ_{org} = 17% w/w_{total}, l = 0.1 mm). Key: open symbols, A'_{λ}, miniemulsions containing **1** (C_1 = 2% w/$w_{monomer}$); full symbols, $A'_{0,\lambda}$, PI-free miniemulsions. d_d: 84 nm (□, ■), 79 nm (◇, ◆), 70 nm (Δ, ▲), 65 nm (○, ●), and 60 nm (☆,★).

where

$\Sigma_\lambda P'_{a,\lambda}$: absorbed polychromatic photon flux in the heterogeneous system [einstein L^{-1} s^{-1}]

$\Sigma_\lambda P_{s,\lambda}$: scattered polychromatic photon flux in the heterogeneous system[54] [einstein L^{-1} s^{-1}]

$$\sum_{\lambda}(P'_{a,\lambda} + P_{s,\lambda}) = \sum_{\lambda} P_{0,\lambda}(1 - e^{-N\sigma_\lambda l}) = \sum_{\lambda} P_{0,\lambda}(1 - e^{-N(\sigma_{a,\lambda} + \sigma_{s,\lambda})l}) \quad (5)$$

N: number density of droplets (or particles) [m^{-3}]

σ_λ: the overall cross section [m^2]

$\sigma_{a,\lambda}$: absorption cross section [m^2]

$\sigma_{s,\lambda}$: scattering cross section [m^2]

Given the negligible absorption characteristics of the acrylate monomers, SDS and hexadecane in the wavelength range of excitation applied, $P_{a,\lambda}$ and $P'_{a,\lambda}$ in eqs 2 to 5 imply the absorption by the PI only. If the droplet size in a dispersed system is decreased, overall scattering ($\Sigma_\lambda P_{s,\lambda}$) is expected to diminish and would lead primarily to a higher transparency of the system ($\Sigma_\lambda P_{t,\lambda}$). However, based on the preservation of the overall mass of organics and assuming the same component distribution in smaller droplets, a reduction of droplet size would increase the number density of droplets (N) and, in accord with eq 5, an increase of $\Sigma_\lambda P'_{a,\lambda}$.

Spectrophotometric analysis is used to record internal transmittance T_λ, eq 6, that is related by Lambert−Beer's law to the product of [PI], $\varepsilon_{PI,\lambda}$ and l:

$$T_\lambda = \frac{P_{t,\lambda}}{P_{0,\lambda}} = 10^{-\varepsilon_{PI,\lambda}[PI]l} \quad (6)$$

Absorbance A_λ is defined as the decadic logarithm of the inverse value of T_λ and represents therefore the product of [PI], $\varepsilon_{PI,\lambda}$ and l (eq 7),

$$A_\lambda = \log\frac{1}{T_\lambda} = \varepsilon_{PI,\lambda}[PI]l \quad (7)$$

In a similar way, the internal transmittance T_λ of a given sample of PI dissolved in a heterogeneous system may be derived from eqs 5 and 6 as

$$T_\lambda = \frac{P_{t,\lambda}}{P_{0,\lambda}} = 10^{-(\sigma_{s,\lambda}Nl + \sigma_{a(PI),\lambda}Nl)} \quad (8)$$

leading to eq 9 to define the apparent absorbance A'_λ

$$A'_\lambda = \log\frac{1}{T_\lambda} = \sigma_{s,\lambda}Nl + \sigma_{a(PI),\lambda}Nl = A'_{s,\lambda} + A'_{a,\lambda} \quad (9)$$

where $A'_{s,\lambda}$ and $A'_{a,\lambda}$ describe respectively the apparent absorbance due to absorption and droplet scattering. Figure 1 shows the absorption spectra of monomer miniemulsions of different average droplet sizes (60 to 84 nm) including **1**. They clearly show that the apparent absorbance of these dispersed systems is the combined result of both absorption and light scattering. The λ_{max} (310 nm) of the absorption band of the n,π^*-transition of **1** dissolved in the miniemulsions is practically unchanged from that found in acetonitrile solution (314 nm).

PI-free miniemulsions do not absorb in the UV−C to UV-A spectral regions, and eq 9 can be simplified to eq 10

$$A'_{0,\lambda} = \sigma_{s,\lambda}Nl = A'_{s,\lambda} \quad (10)$$

Since the light-absorbing component (PI) represents less than 3% of the mass of the miniemulsion and is of negligible effect on the refractive index of the dispersed phase, it may be assumed that the same $\sigma_{s,\lambda}$ could be used in eqs 9 and 10. Applying the same homogenization procedure to PI-free formulations, non-absorbing miniemulsions with similar droplet size distributions (60−84 nm) and comparable N were produced. PI-free monomer droplets are only scatterers as shown by the absorption spectra related by Figure 1. Given the small droplet radii compared to the wavelengths of the scattered light, the experimentally determined scattering cross-section $\sigma_{s,\lambda}$ appears to be proportional to λ^{-4} (Raleigh[54]).

Comparison of the apparent absorbance of miniemulsions of similar droplet size with (eq 9) and without **1** (eq 10) gave access to the values of A'_s, A'_a at 310 nm (λ_{max}), which are displayed in Table 1 for l = 0.1 mm. Also reported is the single-scattering ratio ω_λ corresponding to the experimentally determined absorbance due to scattering (PI-free miniemulsions) divided by the apparent absorbance of PI-containing miniemulsions (i.e., absorption

Table 1. Experimentally Determined Apparent Absorbances (A'_{310}) and Calculated Absorbances Due To Absorption ($A'_{a,310}$) of Miniemulsions (φ_{org} = 17% w/w_{total}) Containing 1 (C_1 = 2% (w/$w_{monomer}$)) as Well as Experimentally Determined Absorbances Due To Scattering ($A'_{s,310}$) of PI-Free Miniemulsions and Single-Scattering Ratio ω_{310} as a Function of the Average Droplet Diameter (d_d), l = 0.1 mm

d_d, nm	A'_{310}	$A'_{s,310}$	$A'_{a,310}$	ω_{310}
84	3.0	1.24	1.8	0.40
79	2.9	1.03	1.9	0.34
70	2.8	0.88	1.9	0.32
65	2.6	0.68	1.9	0.27
60	2.5	0.55	1.9	0.24

Scheme 3. Structures of Photochemical Initiators (PI) 2 (Water-Soluble) to 5

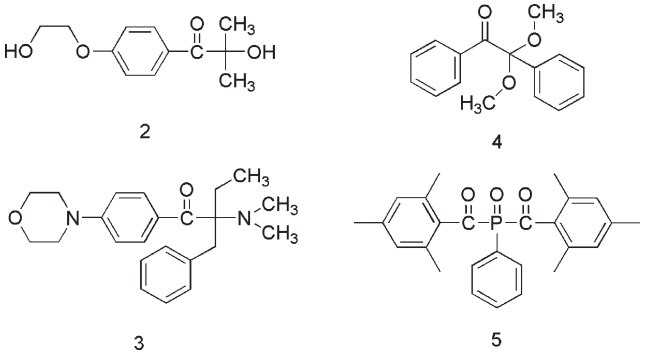

plus scattering) at a given wavelength of excitation (eq 11).

$$\omega_\lambda = \frac{A'_{s,\lambda}}{A'_{s,\lambda} + A'_{a,\lambda}} \tag{11}$$

The values of apparent absorbance (A'_{310}) decrease with decreasing d_d entirely due to the dependence of $A'_{s,310}$ on d_d (Table 1). By contrast, the results relate a practically constant $A'_{a,310}$ within this short-range of d_d. The interplay of nearly constant $A'_{a,310}$ and diminishing $A'_{s,310}$ values yields a single-scattering ratio (ω_{310}) decreasing from 0.4 at 84 nm to only 0.24 at 60 nm. Consequently, the apparent absorption at 310 nm of these smallest monomer droplets (60 nm) is largely dominated by absorption ($A'_{a,310}$). Within the experimentally chosen range of d_d (<100 nm) and with C_1 = 2% (w/$w_{monomer}$), absorption measurements were limited to l = 0.1 mm, yet, already at this optical path length, A'_{310} values exceed 1.5. Consequently an analysis of larger miniemulsion droplets (d_d > 100 nm) was not feasible, and the observed slight decrease of $A'_{a,310}$ with larger d_d cannot be verified. Evidently, for smaller droplets (d_d < 60 nm), light scattering could be further minimized by using microemulsions (20−50 nm) instead of miniemulsions. However, such systems would be severely mass limited, and the resulting product difficult to isolate and purify. Therefore, in order to take full benefit of the advantages of miniemulsions, the diameter of the droplets (d_d) and the concentration of PI should be varied to obtain a satisfactory ratio of absorption to scattering values.

Though we were aware of the difficulties to relate the absorbance data of dispersed and homogeneous systems, the absorption component of the apparent absorbance ($A'_{a,310}$) was nevertheless compared with the absorbance $A_\lambda = [PI]\varepsilon_{PI,\lambda}l$ of **1** determined in solution under equal conditions (λ_{max}, l, C_1, and [**1**]). The calculated $A'_{a,310}$ values of **1** solvated in miniemulsions (1.8−1.9) matched relatively well the absorbance A_{314} (1.9) found with a solution of **1** in acetonitrile. Interestingly, absorption spectra of other conventional lipophilic PIs (**3** to **5**; see Scheme 3) show equally good fits between $A'_{a,\lambda_{max}}$ values, obtained with miniemulsions of d_d = 60 nm, and $A_{\lambda_{max}}$ values in corresponding acetonitrile solutions (Table 2). The overall result implies that the UV absorption properties of the PIs investigated are not affected by their higher local concentration within the lipophilic phase of the miniemulsion. This result also implies that each single droplet may be seen as a suitable "nano-photoreactor", nevertheless under conditions, where excitation is attenuated by scattering.

Table 2. Comparison between Calculated Absorbances Due To Absorption ($A'_{a,\lambda_{max}}$) of Miniemulsions (φ_{org} = 17% w/w_{total}) Containing 1, 3, 4 and 5, Respectively (C_{PI} = 0.34% w/$w_{organic\ and\ aqueous\ phase}$), and Absorbances of the Same PIs in Acetonitrile Solution ($A_{\lambda_{max}}$) ([PI] = 0.34% w/$w_{acetonitrile}$ in Solution), l = 0.1 mm

PI	$A'_{a,\lambda_{max}}$ (miniemulsion)	$A_{\lambda_{max}}$ (solution)
1	1.9	1.9
3	1.9	2
4	0.04	0.04
5	0.6	0.7

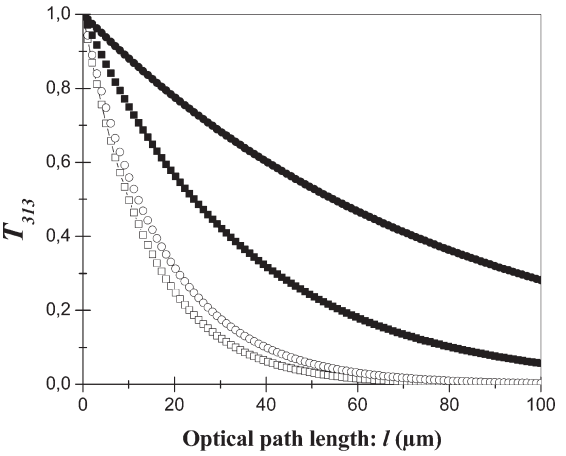

Figure 2. Transmittance (T_{313}) of monomer miniemulsions (φ_{org} = 17% w/w_{total}) as a function of l. Key: open symbols, miniemulsion containing **1** (C_1 = 2% w/$w_{monomer}$); full symbols, PI-free miniemulsions. d_d: 84 nm (□, ■), 60 nm (○, ●). λ_{exc}: 313 nm.

Dealing with the technical issues of photopolymerization in miniemulsions, the very high $A'_{\lambda_{max}}$ values in the UV spectral region represent a real challenge. For acrylate miniemulsions containing **1**, $A'_{\lambda_{max}}$ values were found to vary from 250 to 300 (Table 1, l = 1 cm) and, as shown in Figure 1, less than 50% (d_d = 60 nm) of the apparent absorption is due to scattering. This is primarily due to C_{PI}, and it may be assumed optimal values of C_{PI} would be considerably lower taking into account the compartmentalization of the PI and the space limited diffusion of radicals within the "nanoreactor".

Under the present experimental conditions, penetration of radiation into miniemulsions with $A'_{\lambda_{max}}$ values approximately 250 would not exceed 100 μm (Figure 2). Figure 2 illustrates the transmittance at 313 nm (T_{313}) as a function of l (a strong emission line of the Hg−Xe arc) for miniemulsions containing **1**, assuming that Lambert−Beer's law would be valid. However, deviation from Lambert−Beer's law is obvious due to the high values of C_1 and N. Nonetheless, this simple approximation on the basis of Lambert−Beer's law still yields useful data: with droplet sizes between 60 and 84 nm, more than 95% of the incident radiation is estimated to be absorbed within the first 55 and 40 μm of l into the reaction system, and a very strong heterogeneity between irradiated and nonirradiated volume is to be expected. Only a small fraction of droplets close to the irradiated reactor surface is in fact irradiated. The simple model reveals for PI-free miniemulsions a much larger irradiated volume

dx.doi.org/10.1021/ma201753d |*Macromolecules* 2011, 44, 8727–8738

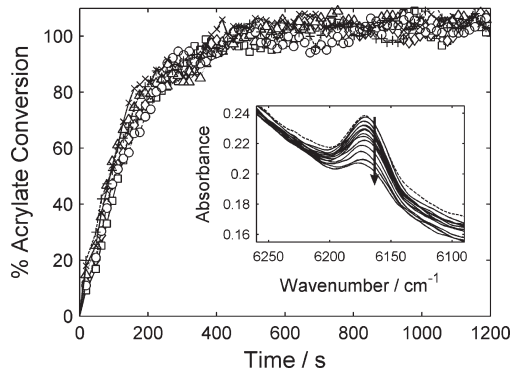

Figure 3. Evolution of the acrylate photopolymerization initiated by **1** in miniemulsions of different d_d. Droplet diameters (d_d): 98 nm (□), 84 nm (◊), 79 nm (Δ), 70 nm (○), 65 nm (×), and 60 nm (+). (Exitance E_p: 100 mW/cm^2, φ_{org} = 17% w/w_{total}.) Inset: evolution of the absorption band of the acrylate π-bond at 6170 cm^{-1} during the first 200 s of irradiation.

and, hence, confirms the need for an optimization of C_{PI}. Although the "shielding" effect was found to be substantially reduced compared to highly scattering micrometrically sized macromemulsions, light scattering may still be considered to be a significant obstacle for a technical development of corresponding polymerization processes. Concern arises in particular, because miniemulsion photopolymerization is expected to take place at higher optical paths (≥1 mm) than conventional UV-cross-linking of static films (1−100 μm). Therefore, optimization of C_{PI} as a function of d_d will be one of the key issues of further technical development. Nevertheless, under optimized technical conditions, smaller optical paths may be partially compensated by irradiating high turbulent reaction systems, taking into account that miniemulsion polymerization is macroscopically viscosity independent of the molecular weight of the polymer to be produced.

II. Radical Photopolymerization in Miniemulsions: Reaction Kinetics, Molar Masses, and Colloidal Properties. The kinetics of the photochemically initiated polymerizations were monitored *in situ* by RT-FTNIR. This technique provides fast temporal resolution and compatibility with complex reaction systems containing high concentrations of water that obstructs the mid-infrared spectral region usually employed for monomer quantification. In a typical experiment, the miniemulsion contained in a quartz cell (l = 1 mm) was exposed simultaneously to an analyzing NIR and an exciting UV beam, this latter exiting from a waveguide. This real-time technique is usually implemented for the online monitoring of the photochemically initiated cross-linking of static films[55] and has so far never been described for emulsion polymerization. RT-FTNIR allowed the continuous quantification of the monomer consumption throughout UV-irradiation by monitoring the diminution of absorbance of the characteristic acrylate π-bond[56] centered at 6170 cm^{-1}. In addition to reaction kinetics, issues of nucleation mechanism and polymer quality (molar mass, polydispersity) were also addressed by focusing on the effects of three experimental parameters: initial d_d, $\Sigma_\lambda P_{0,\lambda}$, and the nature of PI.

Effect of Initial Monomer Droplet Size (d_d). The evolution of radical polymerization of acrylate miniemulsions containing **1** as a function of d_d is shown in Figure 3, where the normalized acrylate conversion is plotted against irradiation time. Different d_d values between 60 and 100 nm were obtained by adjusting the sonication time, the lower limit representing the minimum value that could be achieved with the chosen reaction system. The higher limit was imposed by the decreasing transparency in the NIR spectral region, necessary to ensure satisfactory signal detection. All curves present the same profile and exhibit a quasi-constant initial rate of polymerization (r_p) during the first 3 min of irradiation that led to approximately 70% conversion. Total conversion was reached within about 450 s at slower rates. It might be assumed that the similarity of these curves reflects equivalent reaction kinetics and no changes of the UV-absorption characteristics due to a variation of d_d. The screening effect by light scattering, although dependent on d_d (see Table 1 and Figure 2), appeared to be practically ineffective on the course of the polymerization in 5 different miniemulsions. This might be explained by the fact that the incident photon flux is totally absorbed within less than 100 μm of optical path, i.e., within a distance, where definitely smaller scattering values varying by a factor of about 2 (Table 1) are apparently no longer significant. The similarity of the curves might also be a strong argument for a diffusion controlled polymerization in a reactor without stirring. The marked screening effect observed in miniemulsions with l = 1 mm (Figure 2) does not prevent the course of the reaction as long as the diffusion of the monomer droplets in the whole volume of a spectroscopic cell is ensured, even in the absence of stirring. In the absence of PI, no polymerization could be observed under the experimental conditions employed, this result giving evidence that neither acrylate photolysis nor heat-activated reaction would take place (temperature of the reaction system during irradiation: 25 °C). One final note is that the impact of droplet diameter was only assessed within a very narrow range (60−90 nm). Such conditions are not favorable for observing a compartimentalization effect. Segregational effects between discrete particles leading to faster rates of radical polymerization are generally observed, when the droplet size of monomer miniemulsions is decreased.

Table 3. Effect of Droplet Size (d_d) and Exitance (E_p) on Colloidal Properties (d_p, N_p/N_d), Reactions Kinetics ($r_p^{rel}(1)$, $t_{100\%}$), and the Polymer Characteristics (Number Average Molar Mass (M_n) and Polydispersity Index (M_w/M_n)) During the Acrylate Photopolymerization Initiated by 1 in Miniemulsions of Different d_d

E_p, mW/cm^2	d_d, nm	d_p, nm	N_p/N_d	$r_p^{rel}(1)$[a]	$t_{100\%}$,[b] s	M_n, 10^3 g/mol	M_w/M_n
200	98	82	1.40	1	450	64.9	2.51
200	84	72	1.33	1	450	-	-
200	79	68	1.28	1	450	39.5	3.04
200	70	65	1.02	1	450	-	-
200	65	59	1.06	1	450	-	-
200	60	56	1.00	1	450	36.3	2.75
50	79	66	1.44	0.88	450	51.2	4.53
10	79	59	1.97	0.64	500	82.5	5.78
4	79	57	2.16	0.50	650	174	4.42

[a] See eq 1, reference rate taken with miniemulsion of d_d = 98 nm. Reference results: first line of Table 3. [b] $t_{100\%}$: time necessary to reach complete conversion.

Table 3 provides additional data on colloidal properties and molar masses of the resulting polymer latexes. A relatively good correspondence between droplet (d_d) and particle size (d_p) was found for all d_d investigated, however, d_p was in all cases slightly

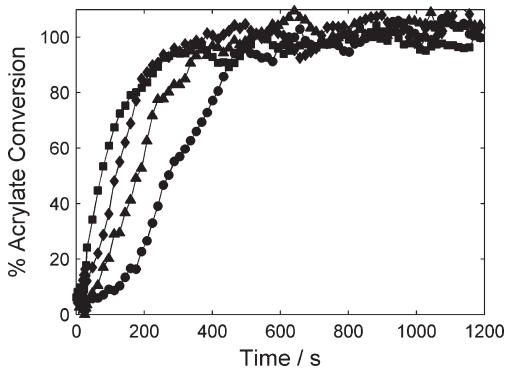

Figure 4. Effect of the exitance (E_p) on the evolution of the acrylate photopolymerization in miniemulsions containg **1** (φ_{org} = 17% w/w_{total}, d_d = 79 nm). E_p: 200 mW/cm^2 (■), 50 mW/cm^2 (◆), 10 mW/cm^2 (▲), and 4 mW/cm^2 (●).

smaller than d_d of the corresponding monomer system. The differences might be due, at least in part, to a shrinkage caused by the change in density during the monomer to polymer transformation ($\gamma_{monomer}$ = 0.933 g/cm^3, $\gamma_{polymer}$ = 1.13 g/cm^3 (average from polybutyl acrylate and poly(methyl methacrylate) tabulated mass densities).[57]

The ratio of the number of particles to that of droplets (N_p and N_d, respectively) was calculated taking into account the density of each phase. The ratio N_p/N_d decreased steadily with the decrease of the initial droplet size d_d, and, at the same time, the difference between d_d and d_p was getting smaller. For droplet sizes above 70 nm, N_p/N_d ratio is higher than 1, which is indicative of the generation of new particles. Such result could be explained by homogeneous or micellar nucleation in the aqueous phase. From 50 to 100 nm, the total surface area formed by the droplets varies from 2.2 × 10^{22} to 1.0 × 10^{22} nm^2/L. These values were found to be in the same range or higher than the estimated interfacial area occupied by SDS molecules (taking a parking area of 0.4 nm^2/molecule[58]): 1.2 × 10^{22} nm^2/L. This result shows that the probability of having micelles (micellar nucleation) is limited at high droplet size and impossible at low droplet size.[59] The high proportion of MMA in the organic phase with its relatively high water-solubility (1.6 g/L) may contribute to the fraction of radicals that precipitates in the aqueous phase producing particles by homogeneous nucleation. As d_d deceases, less surfactant molecules would be available in the bulk aqueous phase for the stabilization of particles produced by homogeneous nucleation. The resulting higher surface area with decreasing d_d of the droplets may in contrast favor the entry of oligoradicals into the monomer droplets, thereby increasing the fraction of particles generated by droplet nucleation. However, one must bear in mind that similarities in N_d and N_p do not necessarily imply that droplets of monomers just turn into polymer particles in a "one-to-one copy" fashion.

In order to complement the characterization of the latexes produced, size exclusion chromatography (SEC) was employed to determine the number-average molar mass, M_n and the polydispersity index, M_w/M_n. The available data (Table 3) confirm that there is no clear effect of droplet size on polymer molecular weight.

Effect of Exitance (E_p). A variation of E_p (between 4 to 200 mW/cm^2) led to significant changes of the rates of monomer conversion. From the kinetic profiles depicted in Figure 4 for acrylate photopolymerizations in miniemulsions of d_d = 79 nm, two main parameters were extracted and displayed in Table 3: $t_{100\%}$ and r_p^{rel}. When decreasing E_p from the reference value (200 mW/cm^2) to 4 mW/cm^2, r_p^{rel} dropped to 0.5, and the observed decrease of r_p^{rel} does not correspond to the conventional scheme of photopolymerization, for which the rate of polymerization scales with the square root of E_p. A smaller local concentration of initiating radicals per unit time will lead to a longer time for eliminating dissolved molecular oxygen and monomer inhibitors.[60]

It is interesting to note that low values of E_p induced periods of initiation that got more pronounced as E_p dropped below 20 mW/cm^2, and this observation might be taken as further qualitative evidence for the presence of two parallel nucleation mechanisms. A decrease of E_p led at the same time to an increasing N_p and to an increasing difference $d_d - d_p$ (from 11 to 22 nm) as d_p decreased steadily. All results are still in agreement with the presence of droplet polymerization, the importance of which diminishes as the rate of polymerization decreases in favor of homogeneous nucleation. In fact, at lower E_p, lower local concentrations of initiator radicals and, subsequently of living polymer, are produced. Propagation of polymerization is mainly represented by the slopes of the conversion curves represented in Figure 3 for conversions between 0 and 70% and in Figure 4 for conversions between 0 to 20 and 80%, respectively, the lower value depending on E_p. Increasing times until propagation is started may be due to low (insufficient) local radical concentrations. As a consequence of longer nucleation periods, the latexes produced at low exitance are broader in size.[61] However, the relationship between longer polymerization times encountered at low exitance and the higher propensity to homogeneous nucleation is difficult to explain.

The molar mass M_n increased markedly with the decrease of E_p, rising from 39.5 × 10^3 (200 mW/cm^2) to 174 × 10^3 g/mol (4 mW/cm^2). The result reflects the diminishing importance of radical−radical, *i.e.*, living polymer, reactions terminating propagation. The slow evolution of the polymerization at conversions exceeding 80% evidence the rather long lifetime of the living polymer. The multiplicity of the nucleation loci and the mixed mode of particle nucleation at lower exitance leads to a significant broadening of the molar mass distribution, which is consistent with the broader latex particle size distributions produced from these miniemulsion polymerizations.

Effect of the Nature of the PI. In addition to **1**, the efficiency of several type I photochemical initiators (Scheme 3) was studied. PI **3** represents another α-aminoacetophenone-type initiator with an electron-donating substituent in the *para*-position, changing the electronic excitation from a n,π* (**1**) to a charge transfer transition. Initiators **2** and **4** belong to the group of α-hydroxyl or α-alkoxyl substituted acetophenones, the α-substitutents focusing, like the α-amino group, on the stabilization of the C-centered radical generated by the type I reaction (Scheme 1). The ethylene glycol substitutent in the *para*-position has no decisive effect on the excited state reactivity of **2**, but provides the solubility of the compound in water (**2** was dissolved in the aqueous reaction system before irradiation). Acylphosphine oxide type initiators are represented with **5**.

In all cases, electronic excitation and subsequent α-cleavage yield benzoyl radicals that add with similar rate constants (k_{add}) to *n*-butyl acrylate (average k_{add} (acetonitrile): 5 × 10^5 M^{-1} s^{-1}[62]). The corresponding rate constants of the parent α-aminoalkyl

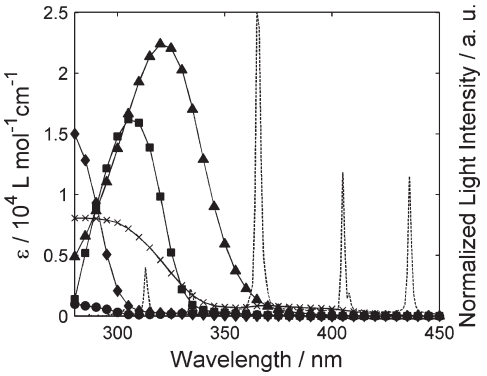

Figure 5. Absorption spectra of **1** (■), **2** (◆), **3** (▲), **4** (●), and **5** (×) in acetonitrile and normalized emission spectrum of a Hg−Xe lamp equipped with a borosilicate filter.

(generated from **1** and **3**) and 2-hydroxy-2-propyl (generated from **2**) radicals, generated by the type I reaction, are about 10 to 50 times higher than those of the benzoyl radicals. The 1, 1-dimethoxy-benzyl radicals (generated from **4**) are known to fragment into methyl benzoate and methyl radicals, the latter enhancing the concentration of living polymers. The photolysis of the phosphine oxide derivative **5** yields, besides benzoyl radicals, the corresponding P-centered radical for which a k_{add} of 2.8×10^7 $M^{-1}s^{-1}$ was measured in acetonitrile solution of *n*-butyl acrylate.[62]

The absorption spectra of this series of initiators is displayed in Figure 5, together with the spectral emission of a Hg−Xe lamp equipped with a borosilicate filter (λ > 300 nm). The emitted polychromatic radiant energy (I_0) within a defined spectral range may be taken from publications of the producer.[63] Emitted incident spectral radiant energies ($I_{0,\lambda}$) might also be available from the same sources or can be calculated on the basis of the polychromatic radiant energy and the spectral distribution of the radiative source (Figure 5). Absorbed radiant energies may then be calculated for given wavelengths ($I_{abs,\lambda}$) or spectral ranges (I_{abs}) using eqs 12 or 13. In the present work, values of I_{abs} were calculated for the spectral region of 300 to 450 nm and normalized (I_{abs}^{rel}) to that of PI **1**.

$$I_{abs,\lambda} = I_{0,\lambda}(1 - 10^{-A_\lambda}) \quad (12)$$

$$I_{abs} = \int_{\lambda_1}^{\lambda_2} I_{0,\lambda}(1 - 10^{-A_\lambda})\, d\lambda \quad (13)$$

The resulting I_{abs}^{rel} were as follows: **2** (0.39), **4** (0.74), **1** (1), **3** (2.07), and **5** (2.36). Compared to the spectra of the nonsubstituted (**4**) or alkoxy-substituted (**2**) compounds, the strong electron donating character of the aromatic alkyl sulfide (**1**) and morpholino (**3**) substituents results in red-shifted absorption maxima, appropriate for exploiting the emission lines of Hg at 313 and eventually at 367 nm. Within the spectral range investigated, the bisacylphosphine oxide **5** exhibits lower ε-values than compounds **1** to **4**, but its absorption is extended into the Vis spectral region. The additional overlap with the Hg-emission lines at 407 and 435 nm contributes to the highest I_{abs} calculated among the initiators investigated. The I_{abs} values of PI **1** to **5** were calculated based on spectral data using acetonitrile as a solvent, and changes in polarity of the solvating environment and scattering effects might affect these values, when these PIs are dissolved in heterogeneous reaction systems.

Table 4. Relative Absorbed Radiant Energies (I_{abs}^{rel}), Quantum Yields of Primary Radical Generation (Φ_α) and $r_p^{rel}(1)$ Determined for the Photochemically Initiated Polymerization of Acrylates in Miniemulsions Using Photochemical Initiators 1 to 5 (E_p = 200 mW/cm^2, d_d = 60 nm)

PI	I_{abs}^{rel}	Φ_α	$r_p^{rel}(1)^a$ s^{-1}	Conversion (t = 1800 s) %
1	1	0.13	1	100
2	0.39	0.29	0.93	100
3	2.07	0.24	0.23	100
4	0.74	0.52−1	1.2	75
5	2.36	0.5−0.7	1.6	30

[a] See eq 1, dd =60 nm, reference data ($r_p^{200mW/cm2}(1)$): first line of Table 3.

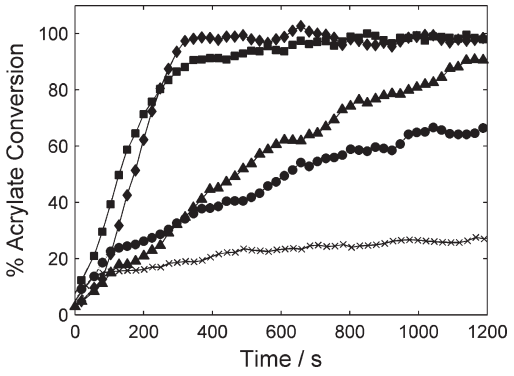

Figure 6. Conversion of acrylate miniemulsions (φ_{org} = 17% w/w_{total}, d_d = 60 nm) containing PI **1** to **5**, respectively, as a function of the irradiation time (concentration of **1** (■), **2** (◆), **3** (▲), **4** (●), and **5** (×): 2% w/$w_{monomer}$. E_p: 100 mW/cm^2).

Table 4 shows important differences of rates of polymerization in miniemulsions of equal d_d depending on the PI used. A variation of d_d (60−100 nm) had only a minor effect on the reaction kinetics (not represented), regardless of the nature of the PI.

The evolution of monomer acrylate consumption during photoinitiated polymerization under similar irradiation conditions is plotted for PI **1** to **5**, respectively, in Figure 6. Polymerization experiments with **1** and **2** reached full conversion of the monomer within less than 20 min. In contrast, experiments with **3** needed about 30 min to complete polymerization, and for miniemulsions containing **4** and **5** incomplete conversions of 75 and 30%, respectively, were observed. Table 4 summarizes the relative apparent polymerization rates (r_p^{rel}). In the experiments with **2**, r_p values were found equal and only slightly lower than those obtained with **1**. In contrast, experiments with **3** resulted in a reactivity far below of the former ones. Norrish type II-reactions might be possible from a n,π^*-triplet state,[64] but it seems more likely that the polar charge transfer excited state already mentioned is solvated and deactivated in the polar periphery of monomer droplets. With initiators **4** and **5**, r_p^{rel}-values are markedly smaller than those found in the reference experiment (using **1**), and, in addition, conversions remained incomplete. In addition, and in contrast to the photoinitiating systems **1**, **2** or **3** where r_p^{rel}-values decrease with decreasing exitance (illustrated in Figure 4 for **1** only), the pattern was found to be more complex for the systems containing **4** or **5** (Figure 7).

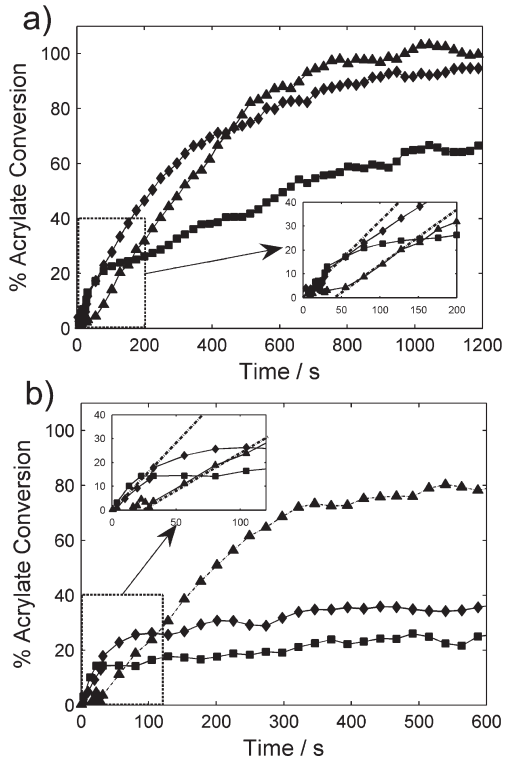

Figure 7. Acrylate miniemulsion conversion in function of irradiation time in presence of PI **4** (a) and **5** (b), respectively. ($C_{4\text{ or }5}$ = 2% w/$w_{monomer}$, d_d = 75 nm, φ_{org} = 17% w/w_{total}. E_p: 200 mW/cm^2 (■), 20 mW/cm^2 (◆) and 4 mW/cm^2 (▲).

When E_p is increased from 4 to 200 mW/cm^2, the final conversion of acrylate in miniemulsions initiated by the benzyl ketal system **4** decreases from 100 to 60%. At the same time, the rate of propagation decreased, as exitance reached 200 mW/cm^2. The evolution was even more pronounced with the reaction systems initiated by **5**. Such kinetic behavior may be related in both cases to a very high local radical concentrations resulting from the combined effect of important Φ_α, very high absorbance values and longer lifetimes of primary radicals. The generation of high local concentrations of primary radicals (α-cleavage of the PI) of relatively long lifetimes within a restricted space and short time of irradiation[65,66] will in fact lead to enhanced termination reactions representing a possible cause for the observed slow rates of polymerization and incomplete conversion. Similar phenomena were reported by Jachuck et al.[7,13] for the continuous photopolymerization of BA in a narrow channel reactor, where high PI concentrations were used, and may be attributed to the competition between monomer and primary radicals for the growing macroradicals. An increased concentration of primary radicals at high exitance contributes to a reduction in the population of macroradicals, thus limiting the number of monomer molecules which could be converted.[66] An interesting feature of the evolutions of acrylate conversion shown in Figures 4, 6, and 7 is that the initial rates of polymerization are quite insensitive toward the power of the incident radiation. Since rates of propagation could only be enhanced by increasing the (local) concentration of initiating radicals or the monomer concentration, the observation indicates that an upper limit of concentration of initiating radicals is already reached at lowest values of exitance

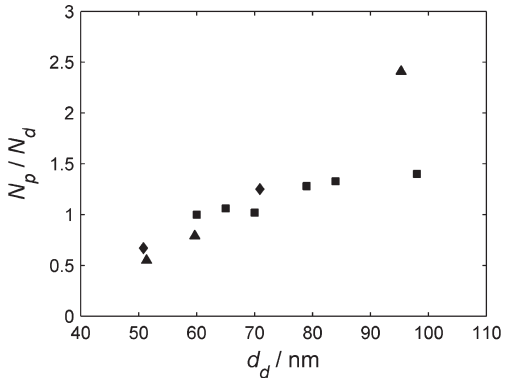

Figure 8. Effect of the initial d_d-value of acrylate miniemulsions on the N_p/N_d-ratio found after photoinitiated polymerization. E_p: 100 mW/cm^2, φ_{org} = 17% w/w_{total}. PI: **1** (■), **2** (◆) and **3** (▲). C_{PI} = 2% w/$w_{monomer}$.

(4 mW/cm^2). Since the local concentration of monomer in acrylate miniemulsions cannot be varied significantly, similar rates are to be expected for initiators generating primary radicals of comparable reactivity.

The influence of the photoiniating system on the nucleation mechanism was also investigated. Previous results showed complete conversion of acrylates, when intitators **1**, **2**, or **3** are used, whereas in miniemulsions containing **4** or **5**, monomer droplets may coexist with particles in incompletely converted systems. Dynamic light scattering data representing the average particle size in a given reaction mixture, is not representative of the actual average size of the produced latex particles. Hence, Figure 8 shows only the dependence of N_p/N_d on d_d for initiating systems leading to complete conversion. Like system **1**, for initial d_d-values above 70 nm, the N_p/N_d-ratio was found to be >1, implying that more polymer particles were generated compared with the initial droplet number. This result is consistent with an increased fraction of particles generated by homogeneous nucleation with larger droplet size as the polymerization is strongly influenced by the presence of hydrophilic functional monomers (MMA, AA). Compared to system **1**, N_p/N_d values further deviating from 1 were obtained with PI **3** and **2**. While the former system is difficult to interpret, the other two can be rationalized given that the number of particles formed by any process other than droplet nucleation is known to increase with the water-solubility of the initiator.[67]

III. Implementation of Photoreactors. Preparative Issues. So far, no reports on a particular design of a photochemical reactor has been published for miniemulsion or emulsion polymerization processes. Pilot or production scale photochemical reactors for liquid monomer polymerization were copied from those used for preparative purposes. Under these conditions, bulk or solution polymerizations face quite often the disadvantage of increasing viscosity or precipitation of the reaction system and, consequently, technical and economical problems due to limited conversions of monomers. In the case of miniemulsion polymerization at restricted organic phase content, viscosity is of no concern. In a first attempt of up-scaling, miniemulsions containing a predefined acrylate monomer mixture (BA/MMA/AA, 49.5/49.5/1% wt., stabilized with SDS and hexadecane) and **1** or **2** (2% w/$w_{monomer}$, the two initiators yielding the highest rates of monomer conversion during laboratory experiments performed in a spectroscopic cell) were irradiated

dx.doi.org/10.1021/ma201753d |*Macromolecules* 2011, 44, 8727–8738

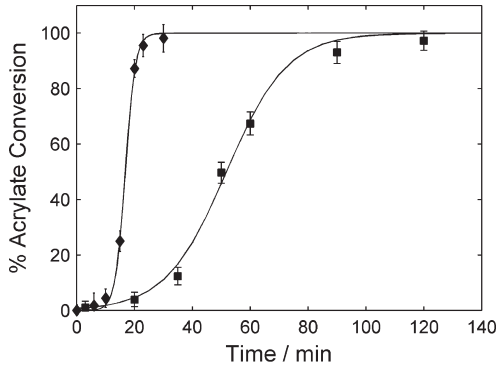

Figure 9. Conversion of acrylate monomers as a function of irradiation time during batch-mode photopolymerization of miniemulsions initiated by **1** (■) or **2** (◆). φ_{org} = 17% w/w_{total}, d_d = 75 nm, $C_{1 \text{ or } 2}$ = 2% w/$w_{monomer}$.

inside an annular photoreactor (400 mL) with a Hg medium pressure arc localized in the reactor axis and inserted into a borosilicate sleeve (Scheme 1).

In batch mode, the photochemical polymerization of the acrylate miniemulsion initiated by **1** reached 50% conversion of the monomer acrylates within 50 min of irradiation time, and conversion was completed after 140 min. The polymerization process was found to be much faster, when **2** was used as initiator, as total conversion was achieved in approximately 40 min of irradiation (Figure 9). The enhanced reactivity of the photoinitiating system **2** may be explained by the overlap of the emission spectra of the two lamps, used with the spectroscopic cell and the annular reactor, respectively, with the absorption spectra of the two initiators. Both arcs (Hg−Xe and Hg medium pressure) exhibit three distinct lines at 302, 313, and 367 nm in addition to the continuum of the Xe-emission in the former (Figure 5). Initiator **1** shows a λ_{max} in the UV−C spectral region with an absorption band spreading up to about 330 nm, whereas the absorption band of initiator **2** (λ_{max}: 308 nm) may reach almost 360 nm. For initiating system **2**, the absorbed radiant power is therefore higher than the one of initiating system **1**.

During these preparative experiments, neither coagulation of the reaction system nor polymer film deposits on the reactor walls could be observed. Relative long induction periods might be attributed to oxygen inhibition, as all experiments were made under normal atmosphere. However, the main advantage of the use of miniemulsions is the achievement of full conversion in batch-mode operation, regardless of the PI employed.

Aiming at the development of a continuous mode for the photoinitiated process of polymerization, semibatch mode polymerizations were conducted using the same photoreactor placed into a linear flow with pump and reservoir. This mode of operation should introduce an enhanced diffusion of radical intermediates with lifetimes of at least microseconds. For thermally initiated emulsion polymerizations, the concept of continuous stirred tank reactors (CSTR) is well-known and has been developed to achieve better polymer quality and lower operational costs.[68,69] Under the present experimental conditions, the initiating system **1** reached within 15 min of irradiation a limit of conversion of 68%, but total conversion was only achieved with initiator **2**.

Polymer characteristics show interesting differences depending on the mode and the nature of the initiator (Table 5).

Table 5. Colloidal Properties and Polymer Molar Mass Obtained for the Miniemulsion Polymerizations Initiated in a Photochemical Reactor (1 or 2)

mode	initiator	d_d/nm	d_p/nm	N_p/N_d	$M_n/10^3$ g/mol	M_w/M_n
batch	**1**	51	75	0.25	242	5.54
batch	**2**	66	70	0.70	261	4.79
continuous	**1**	59	72	0.44	289	3.47
continuous	**2**	66	70	0.68	91.4	8.00

In contrast to earlier experiments in a nonstirred spectroscopic cell, polymerizations in the stirred photochemical reactor produce smaller numbers of polymer particles ($N_p/N_d < 1$) with larger d_p. Since the rate of polymerization is slower in initiating system **1**, the effect of stirring is more pronounced on droplet and particle destabilization. When water-soluble initiator **2** was used, the initial rate of polymerization is enhanced; the effect of stirring on N_p/N_d and d_p is less pronounced. Batch-experiments with **1** and **2** also yield similar M_n-values (2.42×10^5 and 2.61×10^5 g/mol, respectively). Semibatch mode with **2** gave rise to a broad molar mass distribution.

CONCLUSION

The present study reconfirms the feasibility of radical photopolymerization of acrylates in miniemulsion and expands its investigation to the macroscopic optical properties of monomer droplets, reaction kinetics, colloidal properties, and polymer characteristics as well as on their dependence on the operational mode. UV/vis-spectroscopic investigations showed that absorbance characteristics of the initiators are similar between heterogeneous and homogeneous systems, when scattering by droplets within a range of diameters from 60 to 90 nm was taken into account. Absorption spectra of the reaction systems at concentrations inspired by technical formulations indicated total absorbances within a few tens of micrometers of optical path length. Consequently, it was to be expected that the effect of stirring or flow of the reaction system (known to be one of the primary operational parameters in the development of photochemical processes) would be very important, but could not be taken into account for the kinetic investigations made in a nonstirred spectroscopic cell. Investigations based on the FTNIR-analysis of acrylate consumption did not show notable changes of the reaction kinetics of initiating system **1** upon varying the initial droplet size. Expectedly, the initial rate of polymerization depended primarily on the overlap of the spectral absorption of the different initiators investigated with the spectral emission of the radiation sources employed. In addition, the quantum yield of radical generation (mainly by Norrish I) and the solubility (and localization) of the initiator molecules in the heterogeneous reaction system were found to be key factors determining the evolution of the monomer acrylate consumption and the nucleation mechanism. Product formation (initial rate of polymerization, rate of conversion and product characteristics) depends primarily on the average concentration of radical intermediates (primary and oligomer radicals, living polymers). High concentrations of these intermediates lead to a high propensity for radical combination or disproportionation and, hence, to slow rates of polymerization, incomplete conversion and high polydispersity indices. Consequently, radical polymerization in miniemulsion may be optimized primarily by the choice of the nature

of the initiator adapted for a given heterogeneous reaction system and by the incident radiant power or power density to be used.

AUTHOR INFORMATION

Corresponding Author

*E-mail: abraham.chemtob@uha.fr. Telephone: +33 3 8933 5030. Fax: +33 3 8933 5014.

Present Addresses

[†]Department of Chemistry and Chemical Biology, Rutgers, The State University of New Jersey, New Brunswick, NJ 08903.

REFERENCES

(1) Decker, C. *Polym. Int.* **1998**, *45*, 133–141.
(2) Schwalm, R., *UV Coatings Basics, Recent Developments and New Applications*, 1st ed.; Elsevier: Amsterdam, The Netherlands, 2007; p 223.
(3) Melville, H. W.; Chimayanandam, B. R. *Trans. Faraday Soc.* **1954**, 73–80.
(4) Ryan, C. F.; Gormley, J. J. In *Macromolecular Synthesis*; Overberger, C. G., Ed.; John Wiley and Sons: New York: 1963; pp 30−37.
(5) Boutin, J.; Neel, J. US Patent 4,294,676, 1981.
(6) Arndt, P. J. DE Patent 3208369, 1983.
(7) Boodhoo, K. V. K.; Dunk, W. A. E.; Jassim, M. S.; Jachuck, R. J. *J. Appl. Polym. Sci.* **2004**, *91*, 2079–2095.
(8) Dunk, B.; Jachuck, R. *Green Chem.* **2000**, *2*, G13–G14.
(9) Kuriyama, A. US Patent 4,849,183, 1989.
(10) Keggenhoff, B.; Bandtel, E.; Rosenkrauz, H. J. US Patent 4,211,761, 1980.
(11) Teixeira, S.; Giudici, R.; Bossmann, S. H.; Lang, J.; Braun, A. M. *Chem. Eng. Process.* **2004**, *43*, 1317–1328.
(12) Silvares, A. F. M.; Nascimento, C. A. O.; Oliveros, E.; Bossmann, S. H.; Braun, A. M. *Chem. Eng. Process* **2006**, *45*, 1001–1010.
(13) Jachuck, R. J. J.; Nekkanti, V. *Macromolecules* **2008**, *41*, 3053–3062.
(14) Capek, I. *Polym. J.* **1996**, *28*, 400–406.
(15) Capek, I. *Eur. Polym. J.* **1999**, *36*, 255–263.
(16) David, G.; Ozer, F.; Simionescu, B. C.; Zareie, H.; Piskin, E. *Eur. Polym. J.* **2001**, *38*, 73–78.
(17) Jain, K.; Klier, J.; Scranton, A. B. *Polymer* **2005**, *46*, 11273–11278.
(18) Kuo, P. L.; Turro, N. J.; Tseng, C. M.; El-Aasser, M. S.; Vanderhoff, J. W. *Macromolecules* **1987**, *20*, 1216–1221.
(19) Peinado, C.; Bosch, P.; Martin, V.; Corrales, T. *J. Polym. Sci., Part A: Polym. Chem.* **2006**, *44*, 5291–5303.
(20) Pokhriyal, N. K.; Sanghvi, P. G.; Shah, D. O.; Devi, S. *Langmuir* **2000**, *16*, 5864–5870.
(21) Schauber, C.; Riess, G. *Makromol. Chem.* **1989**, *190*, 725–735.
(22) Schweer, J.; van Herk, A. M.; Pijpers, R. J.; Manders, B. G.; German, A. L. *Macromol. Symp.* **1995**, *92*, 31–41.
(23) Wan, T.; Hu, Z. W.; Ma, X. L.; Yao, J.; Lu, K. *Prog. Org. Coat.* **2008**, *62*, 219–225.
(24) Wang, L.; Liu, X.; Li, Y. *Langmuir* **1998**, *14*, 6879–6885.
(25) Wang, L.; Liu, X.; Li, Y. *Macromolecules* **1998**, *31*, 3446–3453.
(26) Capek, I.; Fouassier, J. P. *Eur. Polym. J.* **1997**, *33*, 173–181.
(27) Carver, M. T.; Dreyer, U.; Knoesel, R.; Candau, F. *J. Polym. Sci., Part A: Polym. Chem.* **1989**, *27*, 2161–2177.
(28) Cochin, D.; Candau, F.; Zana, R. *Macromolecules* **1993**, *26*, 5755–5764.
(29) Fouassier, J. P.; Lougnot, D. J. *J. Appl. Polym. Sci.* **1987**, *34*, 477–488.
(30) Fouassier, J. P.; Lougnot, D. J.; Zuchowicz, I. *Eur. Polym. J.* **1986**, *22*, 933–938.
(31) Takeishi, M.; Yoshida, H.; Niino, S.; Hayama, S. *Makromol. Chem.* **1978**, *179*, 1387–1391.
(32) Voortmans, G.; Jackers, C.; De Schryver, F. *Br. Polym. J.* **1989**, *21*, 161–169.
(33) Capek, I. *Macromol. Rep.* **1996**, *A33*, 209–217.
(34) Encinas, M. V.; Rufs, A. M.; Bertolotti, S. G.; Previtali, C. M. *Polymer* **2009**, *50*, 2762–2767.
(35) Hu, X.; Zhang, J.; Yang, W. *Polymer* **2009**, *50*, 141–147.
(36) Liu, L.; Yang, W. *J. Polym. Sci., Part A: Polym. Chem.* **2004**, *42*, 846–852.
(37) Mah, S.; Lee, D.; Koo, D.; Kwon, S. *J. Appl. Polym. Sci.* **2002**, *86*, 2153–2158.
(38) Shim, S. E.; Shin, Y.; Jun, J. W.; Lee, K.; Jung, H.; Choe, S. *Macromolecules* **2003**, *36*, 7994–8000.
(39) Mayoral, J. F.; Levy, M. *J. Polym. Sci., Polym. Chem. Ed.* **1982**, *20*, 2755–2764.
(40) Shim, S. E.; Jung, H.; Lee, H.; Biswas, J.; Choe, S. *Polymer* **2003**, *44*, 5563–5572.
(41) Tonnar, J.; Pouget, E.; Lacroix-Desmazes, P.; Boutevin, B. *Macromol. Symp.* **2009**, *281*, 20–30.
(42) Fuchs, A. V.; Will, G. D. *Polymer* **2010**, *51*, 2119–2124.
(43) Dou, J.; Zhang, Q.; Jian, L.; Gu, J. *Colloid Polym. Sci.* **2010**, *288*, 1751–1756.
(44) Falk, B.; Crivello, J. V. *Chem. Mater.* **2004**, *16*, 5033–5041.
(45) Falk, B.; Crivello, J. V. *J. Appl. Polym. Sci.* **2005**, *97*, 1574–1585.
(46) Asua, J. M. *Prog. Polym. Sci.* **2002**, *27*, 1283–1346.
(47) Qiu, G.; Wang, Q.; Wang, C.; Lau, W.; Guo, Y. *Polym. Int.* **2006**, *55*, 265–272.
(48) Li, J.; Zhu, X.; Zhu, J.; Cheng, Z. *Radiat. Phys. Chem.* **2006**, *75*, 253–258.
(49) Chen, J.; Zhang, Z.; Zhang, Q. *Radiat. Phys. Chem.* **2009**, *78*, 906–909.
(50) Chen, Y.; Liu, H.; Zhang, Z.; Wang, S. *Eur. Polym. J.* **2007**, *43*, 2848–2855.
(51) Wang, S.; Wang, X.; Zhang, Z. *Eur. Polym. J.* **2006**, *43*, 178–184.
(52) Chemtob, A.; Kunstler, B.; Croutxé-Barghorn, C.; Fouchard, S. *Colloid Polym. Sci.* **2009**, *288*, 579–587.
(53) Dietliker, K. *Compilation of Photoinitiators Commercially Available for UV Today*; Sita technology Ltd: Edinburgh, London, 2002.
(54) Cox, A. J.; DeWeerd, A. J.; Linden, J. *Am. J. Phys.* **2002**, *70*, 620–625.
(55) Decker, C.; Moussa, K. *Makromol. Chem.* **1988**, *189*, 2381–2394.
(56) Grinevich, O.; Snavely, D. L. *Chem. Phys. Lett.* **1997**, *267*, 313–317.
(57) Brandrup, J.; Immergut, E. H.; Grulke, E. A.; Grulke, E. A.; Bloch, D., *Polymer Handbook, 4th Edition*. 1999.
(58) The area per SDS molecule at the interface (which is given by the modified Gibbs adsorption equation) depends on the organic phase-water interface. With acrylates and alkanes, the occupied molecular interfacial area is around 40−50 Å: (a) Rosen, M. J. *Surfactants and Interfacial Phenomena*, 2nd ed.; Wiley: New York, 1989. (b) Rehfeld, S. *J. Phys. Chem.* **1967**, *71*, 738–745.
(59) Rodriguez, R.; Barandiaran, M. J.; Asua, J. M. *Macromolecules* **2007**, *40*, 5735–5742.
(60) Decker, C.; Elzaouk, B.; Decker, D. *J. Macromol. Sci., Pure Appl. Chem.* **1996**, *A33*, 173–190.
(61) Miller, C. M.; Sudol, E. D.; Silebi, C. A.; El-Aasser, M. S. *J. Polym. Sci., Part A: Polym. Chem.* **1995**, *33*, 1391–1408.
(62) Dietliker, K. *A Compilation of Photoinitiators Commercially Available for UV Today*; Sita Technology Ltd.: London, 2001.
(63) Refer to Hamamatsu Photonics website: www.hamamatsu.com.
(64) Alberti, A.; Benaglia, M.; Macciantelli, D.; S., R.; Scoponi, M. *Eur. Polym. J.* **2008**, *44*, 3022–3027.
(65) Okamura, S.; Manabe, T. *Polymer* **1961**, *2*, 83–94.
(66) Goodner, M. D.; Bowman, C. N. *Macromolecules* **1999**, *32*, 6552–6559.

(67) Saethre, B.; Mork, P. C.; Ugelstad, J. *J. Polym. Sci., Part A: Polym. Chem.* **1995**, *33*, 2951–2959.
(68) Asua, J. M. *Polymer Reaction Engineering*; Wiley-Blackwell: Oxford, U.K., 2007.
(69) Chen, H. T.; Kuan, C. N.; Setthachayanon, S.; Chartier, P. A. *AIChE J.* **1980**, *26*, 672–675.